frontiers in Astronomy and Space Sciences

ORIGINAL RESEARCH
published: 02 February 2022
doi: 10.3389/fspas.2021.805162

Rotational Rest Frequencies and First Astronomical Search of Protonated Methylamine

*Philipp C. Schmid[1], Sven Thorwirth[1], Christian P. Endres[2], Matthias Töpfer[1†], Álvaro Sánchez-Monge[1], Andreas Schwörer[1], Peter Schilke[1], Stephan Schlemmer[1] and Oskar Asvany[1]**

[1]I. Physikalisches Institut, Universität zu Köln, Köln, Germany, [2]Max Planck Institute for Extraterrestrial Physics, Garching bei München, Germany

We report first laboratory rest frequencies for rotational transitions of protonated methylamine, $CH_3NH_3^+$, measured in a cryogenic 22-pole ion trap machine and employing an action spectroscopy scheme. For this prolate symmetric top molecule thirteen transitions between 80 and 240 GHz were detected in the ground vibrational state, covering $J_K = 2_K - 1_K$ up to $J_K = 6_K - 5_K$ with $K = 0, 1, 2$. Some transitions exhibit noticeable structure that is attributed to internal rotation splitting. As the CN radical and several of its hydrogenated and protonated forms up to methylamine, CH_3NH_2, are well known entities in the laboratory and in space, protonated methylamine, $CH_3NH_3^+$, is a promising candidate for future radio astronomical detection.

Keywords: rotational spectroscopy, protonated methylamine, ion trap, astrochemistry, symmetric top molecule

OPEN ACCESS

Edited by:
André Canosa, UMR6251 Institut de Physique de Rennes (IPR), France

Reviewed by:
Roman Motiyenko, Université de Lille, France
Anthony Remijan, National Radio Astronomy Observatory, United States

****Correspondence:***
Oskar Asvany
asvany@ph1.uni-koeln.de

†Present Address:
Matthias Töpfer, Vinnolit GmbH & Co. KG, Hürth, Germany

Specialty section:
This article was submitted to Astrochemistry, a section of the journal Frontiers in Astronomy and Space Sciences

Received: *29 October 2021*
Accepted: *22 December 2021*
Published: *02 February 2022*

Citation:
Schmid PC, Thorwirth S, Endres CP, Töpfer M, Sánchez-Monge Á, Schwörer A, Schilke P, Schlemmer S and Asvany O (2022) Rotational Rest Frequencies and First Astronomical Search of Protonated Methylamine. Front. Astron. Space Sci. 8:805162. doi: 10.3389/fspas.2021.805162

1 INTRODUCTION

The cyano radical, CN, was one of the first molecules detected in the interstellar medium (McKellar, 1940). It is astrochemically linked to its hydrogenated and protonated forms, most of which have been detected in the interstellar medium, typically in the galactic center source Sgr B2, such as HCN (Snyder and Buhl, 1971), HNC (Snyder and Buhl, 1972; Zuckerman et al., 1972), $HCNH^+$ (Ziurys and Turner, 1986), and $H_2C = NH$ (Godfrey et al., 1973). The terminal product of this hydrogenation series is methylamine, CH_3NH_2, which has been well characterized by laboratory spectroscopy (Ohashi et al., 1987; Ilyushin and Lovas, 2007; Motiyenko et al., 2014) and was first detetcted in Sgr B2 and Orion A in 1974 by Kaifu et al. (1974) and Fourikis et al. (1974).

In interstellar environments, molecules may also occur in their protonated forms, generated by a proton transfer from a proton donor like H_3^+, e.g. $CO + H_3^+ \rightarrow HCO^+ + H_2$. Many of the simpler protonated species have been detected in the interstellar medium, such as HCO^+ (Buhl and Snyder, 1970), N_2H^+ (Turner, 1974), $HCNH^+$ (Ziurys and Turner, 1986) and $HOCO^+$ (Thaddeus et al., 1981), whereas many of the more complex ones so far are only suspected to be present. Examples are $CH_3NH_3^+$, as a product of proton transfer to methyl amine (see, e.g., the KIDA database; Wakelam et al., 2015) or from radiative association of NH_3 and CH_3^+ (Herbst, 1985), but also protonated methanol, $CH_3OH_2^+$ (Jusko et al., 2019), and protonated methane, CH_5^+ (Asvany et al., 2012; Asvany et al., 2015). In particular the latter two molecular ions have not yet been searched for in space because their laboratory microwave spectra are predicted to be quite irregular and still not known.

Following up on our recent work on the high-resolution rotational spectra of CN^+ (Thorwirth et al., 2019a) and $CH_2NH_2^+$ (Markus et al., 2019), in this study, we finally focus on the very last member of the CN hydrogenation/protonation chain, protonated methylamine, $CH_3NH_3^+$. Upon protonation,

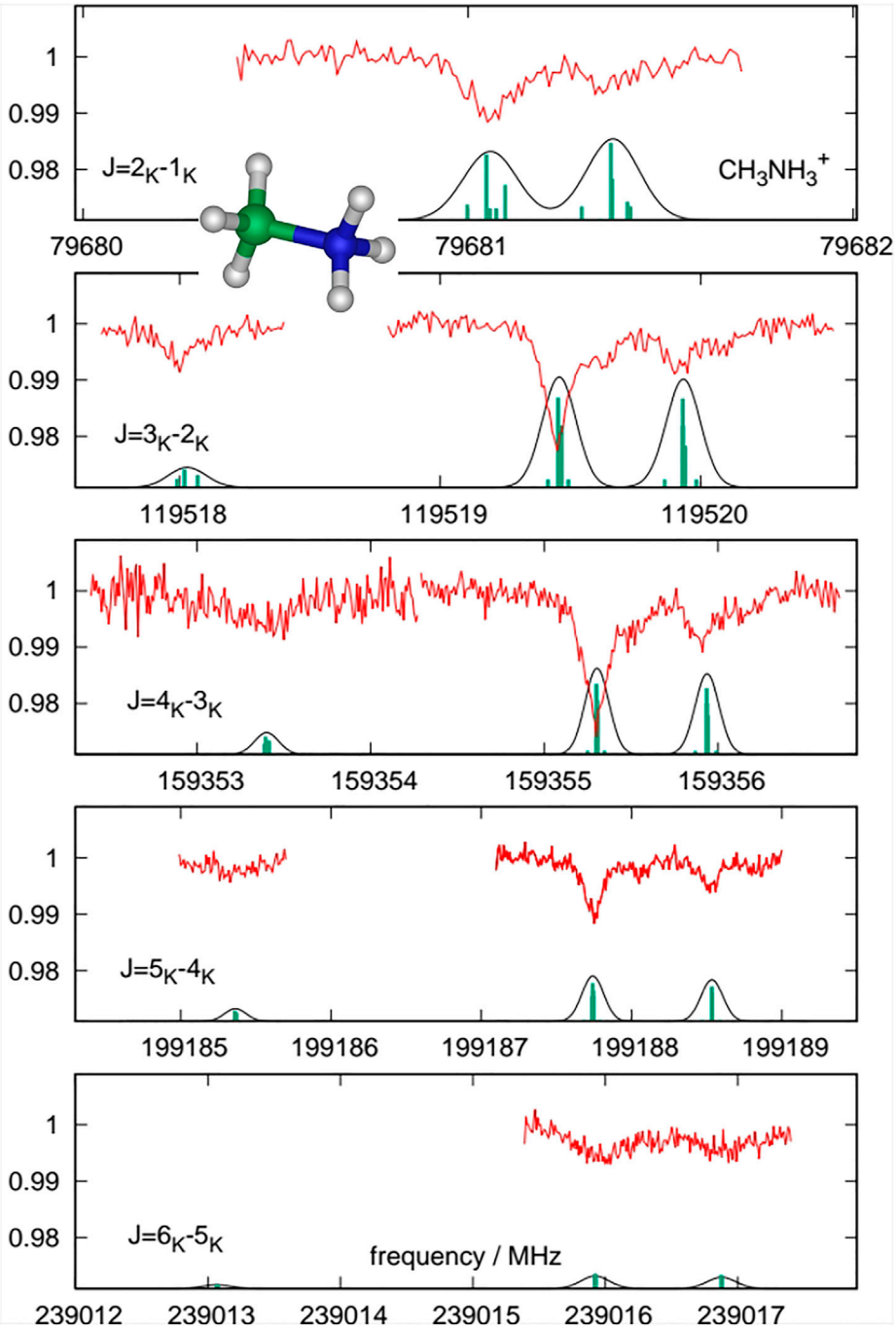

FIGURE 1 | Measurements of the $J'_K \leftarrow J''_K$ (K = 0, 1, 2) rotational transitions of $CH_3NH_3^+$ (red trace), recorded as depletion signal of the normalized $CH_3NH_3^+$–He counts. The simulations (green sticks indicate nitrogen quadrupole hyperfine structure (hfs) and their convolution is given as black traces), based on a symmetric rotor model (**Table 1**, fit I), indicate that the hyperfine splitting is not resolved and that discrepancies between the simulated and measured spectra, in particular the blue-shifted shoulders for K = 0 and 1 (red trace), are most probably due to the neglect of torsional motion in the simulation.

methylamine, CH_3NH_2, an asymmetric top molecule featuring two internal large-amplitude motions (internal rotation and inversion), is converted into a much simpler symmetric top of C_{3v} point group symmetry, in which the CH_3 and the NH_3 groups assume a staggered configuration at the global energy minimum (see inset in **Figure 1**). Literature on the spectroscopy of $CH_3NH_3^+$ is extremely sparse, with only one experimental paper presenting low-resolution infrared (IR) features of the Ar-tagged species (Michi et al., 2003), and one work reporting *ab initio* values for its IR vibrational frequencies (Zeroka and Jensen, 1998). Therefore, the spectroscopic study in the present work was complemented with new high-level quantum-chemical predictions of the

TABLE 1 | Calculated and experimental spectroscopic parameters (in MHz, unless noted otherwise) of $CH_3NH_3^+$. Two experimental fits to the measured data are presented, one (fit I) ignoring the torsional motion, and one (fit II) including torsional motion. Numbers in parentheses are one standard deviation in units of the last digit.

Parameter	C_2H_6		$CH_3NH_3^+$			
	exp.[a]	calc.[b]	calc.[b]	scaled[c]	exp. fit I	exp. fit II[d]
A_e	⋯	81 080.842	85 189.126	⋯	⋯	⋯
B_e	⋯	20 126.248	20 246.782	⋯	⋯	⋯
ΔA_0	⋯	1065.208	1222.937	⋯	⋯	⋯
ΔB_0	⋯	265.982	341.653	⋯	⋯	⋯
A_0	80 391.1(38)	81 080.842	83 966.189	83 251.9	⋯	83 251.9[e]
B_0	19 913.684(24)	19 860.266	19 905.129	19 958.7	19 920.6224(12)	19 941.65(65)
$D_J \times 10^3$	31.026(21)	30.54	34.81	35.4	35.378(27)	35.292(22)
$D_{JK} \times 10^3$	76.37(28)	77.82	84.41	82.8	79.48(38)	87.89(34)
$eQq(^{14}N)$	⋯	⋯	+0.158	⋯	⋯	⋯
μ_e/D	⋯	⋯	2.15	⋯	⋯	⋯
ρ	0.5	⋯	0.54	⋯	⋯	0.54[d]
V_3/kcal/mol	3.00	2.45	1.98	2.42	⋯	2.42[d]
$F \times 10^{-3}$	80.3911[f]	⋯	335.152 576[f]	⋯	⋯	335.152 576[f]
F_{3J}	–397.8(20)	⋯	⋯	⋯	⋯	–243.0(75)
wrms[g]	⋯	⋯	⋯	⋯	1.44	0.96

[a] *see Ozier and Moazzen-Ahmadi (2007) and Borvayeh et al. (2008).*

[b] *This study;* A_e, B_e, $eQq(^{14}N)$ *and dipole moment* μ_e *calculated at the CCSD(T)/cc-pwCVQZ, level, zero-point vibrational corrections* ΔA_0, ΔB_0 *and centrifugal distortion terms calculated at the CCSD(T)/cc-pVTZ, level. Torsional barriers* V_3 *evaluated from the CCSD(T)/cc-pwCVQZ energy difference of the staggered and eclipsed forms complemented with harmonic vibrational corrections evaluated at the CCSD(T)/cc-pVTZ level.*

[c] *Calculated* $CH_3NH_3^+$ *value further scaled with the ratio* X_{exp}/X_{calc} *of the corresponding parameter of* C_2H_6.

[d] *Fit performed using an in-house program assuming a uniform uncertainty of 15 kHz.*

[e] *Kept fixed.*

[f] C_2H_6*: Kept fixed at value of* A *rotational constant;* $CH_3NH_3^+$*: Kept fixed at the customary value of* $A/(\rho(1-\rho))$.

[g] *Weighted rms, dimensionless.*

molecular structure and force field (see **Section 3**). The ion trap experiment is briefly described in **Section 2**. The experimentally derived rotational transitions of $CH_3NH_3^+$ as well as the ground state spectroscopic parameters are summarized in **Section 4**. A first astronomical search of $CH_3NH_3^+$ towards Sgr B2(N) and Sgr B2(M) is finally presented in **Section 5**.

2 EXPERIMENTAL METHODS

The rotational transitions of $CH_3NH_3^+$ have been measured using an action spectroscopic method which exploits the rotational state dependence of the ternary attachment of He atoms to cations at low temperature (Brünken et al., 2014; Brünken et al., 2017; Doménech et al., 2017; Jusko et al., 2017; Doménech et al., 2018a; Doménech et al., 2018b; Thorwirth et al., 2019a; Asvany et al., 2021). The experiment was performed in the 4 K ion trapping machine COLTRAP described by Asvany et al. (2010, 2014). The ions were generated in a storage ion source by electron impact ionization ($E_e \approx 26$–30 eV) of the precursor gas mixture. This mixture consisted of methylamine, CH_3NH_2 (Aldrich Chem. Corporation, CAS 74-89-5, 98%), and helium (Linde 5.0) which were admitted to the ion source via two separate leakage valves. $CH_3NH_3^+$ is generated by a reaction of the type $CH_3NH_2^+ + CH_3NH_2 \rightarrow CH_3NH_3^+ + CNH_4$. A pulse of several ten thousand mass-selected parent ions ($m = 32$ u) was injected into the 22-pole ion trap filled with about 10^{14} cm^{-3} He at 4 K. At the beginning of the trapping time lasting 800 ms, $CH_3NH_3^+$-He complexes formed by three-body collisions with He. The resonant absorption of the cw millimeter-wave radiation by the trapped cold $CH_3NH_3^+$ cations is detected by observing the decrease of the number of $CH_3NH_3^+$-He complexes. A rotational line is thus recorded by repeating these trapping cycles (1 Hz) and counting the mass-selected $CH_3NH_3^+$-He complexes ($m = 36$ u) as a function of the millimeter-wave frequency. This millimeter-wave radiation was supplied by a multiplier chain source (Virginia Diodes, Inc.), covering the ranges 80–125 and 170–1100 GHz. This source was driven by a synthesizer (Rohde&Schwarz SMF100A), which was referenced to a rubidium atomic clock. The beam of the millimeter-wave source has been directed toward the ion trap via an elliptical mirror and a thin diamond vacuum window. The 160 GHz line of $CH_3NH_3^+$ was measured with a different multiplier chain (Radiometer Physics GmbH), covering the range of 110–170 GHz.

3 COMPUTATIONAL METHODS

As no previous high-resolution experimental data were available for $CH_3NH_3^+$, spectroscopic searches and analysis were based on high-level quantum-chemical calculations performed here at the CCSD(T) level of theory (Raghavachari et al., 1989). Equilibrium geometries were calculated using analytic gradient techniques (Watts et al., 1992) and Dunning's correlation-consistent basis sets as large as cc-pwCVQZ (Peterson and Dunning, 2002). Anharmonic force fields to evaluate the zero-point vibrational contributions $\frac{1}{2}\sum_i \alpha_i^{A,B,calc}$ (= ΔA_0, ΔB_0) to the equilibrium

TABLE 2 | Frequencies of pure rotational transitions (in MHz) of $CH_3NH_3^+$, obtained by fitting multiple Gaussians to the spectra in **Figure 1**. The uncertainties (1 σ) are given in parentheses in units of the last significant digits. The assignment of Model I assumes a standard symmetric top Hamiltonian whereas that of Model II assumes a symmetric top featuring torsional splitting, see text for details.

Frequency	Model I				Model II			
	J'_K	←	J''_K	*o* − *c*	J'_K, σ	←	J''_K, σ	*o* − *c*
79681.065(10)	2_1	←	1_1	0.026	2_1,0	←	1_1,0	0.019
79681.364(10)	2_0	←	1_0	0.007	2_0,0	←	1_0,0	0.010
119517.996(10)	3_2	←	2_2	−0.010	3_2,0	←	2_2,0	0.006
119519.449(10)	3_1	←	2_1	0.013	3_1,0	←	2_1,0	0.000
119519.449(10)	⋯	⋯	⋯	⋯	3_1,1	←	2_1,1	0.017
119519.621(10)	⋯	⋯	⋯	⋯	3_1, −1	←	2_1, −1	0.008
119519.908(10)	3_0	←	2_0	−0.005	3_0,0	←	2_0,0	−0.002
119520.077(10)	⋯	⋯	⋯	⋯	3_0, ±1	←	2_0, ±1	−0.006
159353.362(30)	4_2	←	3_2	−0.017	4_2,0	←	3_2,0	0.000
159355.297(10)	4_1	←	3_1	0.011	4_1,0	←	3_1,0	−0.010
159355.297(10)	⋯	⋯	⋯	⋯	4_1,1	←	3_1,1	0.012
159355.537(10)	⋯	⋯	⋯	⋯	4_1, −1	←	3_1, −1	0.011
159355.899(10)	4_0	←	3_0	−0.023	4_0,0	←	3_0,0	−0.023
159356.151(10)	⋯	⋯	⋯	⋯	4_0, ±1	←	3_0, ±1	−0.002
199185.325(30)	5_2	←	4_2	−0.031	5_2,0	←	4_2,0	−0.015
199187.748(10)	5_1	←	4_1	0.008	5_1,0	←	4_1,0	−0.024
199187.748(10)	⋯	⋯	⋯	⋯	5_1,1	←	4_1,1	0.004
199188.039(10)	⋯	⋯	⋯	⋯	5_1, −1	←	4_1, −1	−0.007
199188.518(10)	5_0	←	4_0	−0.017	5_0,0	←	4_0,0	−0.022
199188.820(10)	⋯	⋯	⋯	⋯	5_0, ±1	←	4_0, ±1	−0.009
239016.015(30)	6_1	←	5_1	0.067	6_1,0	←	5_1,0	0.019
239016.931(30)	6_0	←	5_0	0.029	6_0,0	←	5_0,0	0.013

rotational constants were calculated using analytic second-derivative techniques (Gauss and Stanton, 1997; Stanton and Gauss, 2000) followed by additional numerical differentiation to calculate the third and fourth derivatives needed for the anharmonic force field (Stanton et al., 1998; Stanton and Gauss, 2000). These calculations were carried out using the frozen core (fc) approximation in combination with the cc-pVTZ basis set (Dunning, 1989).

All calculations were performed using the CFOUR program (Matthews et al., 2020) and strategies summarized elsewhere (Puzzarini et al., 2010). The computed spectroscopic parameters are listed in **Table 1** that also provides scaled (best-estimate) parameters obtained from a comparison of experimental and calculated values of isoelectronic ethane, C_2H_6 (see, e.g., Martinez et al. (2013) for a similar procedure used in the vinyl acetylene/protonated vinyl cyanide family of isoelectronic species). Additional results from the calculations are given in the **Supplementary Material**. An estimate of the torsional barrier height was obtained using the energy difference between the staggered and the eclipsed forms of $CH_3NH_3^+$ calculated at the CCSD(T)/cc-pwCVQZ level and under consideration of harmonic zero-point vibrational contributions calculated at the CCSD(T)/cc-pVTZ level. This procedure results in a barrier of V_3 = 1.98 kcal/mol. A similar calculation of ethane, C_2H_6, yields 2.45 kcal/mol to be compared against an experimental value of 3.00 kcal/mol (Borvayeh et al., 2008). Using the ethane exp/calc-ratio of V_3 for the purpose of scaling, a best estimate value of 2.42 kcal/mol (846 cm^{-1}) for the torsional barrier in $CH_3NH_3^+$ is obtained.

4 LABORATORY RESULTS AND SPECTROSCOPIC PARAMETERS

Using frequency predictions based on the new high-level quantum-chemical calculations, the lines shown in **Figure 1** were found subsequently during targeted spectroscopic survey scans. The spectra were recorded in individual measurements in which the frequency was stepped in an up-and-down manner several times. The frequency steps were typically 2 kHz, except for the $J_K = 4_K \leftarrow 3_K$ measurement at 159 GHz, for which 10 kHz steps were applied. Such individual measurements were repeated typically ten times. In the depiction of **Figure 1**, all available spectra were accumulated and rebinned to a stepwidth of 10 kHz. This deep integration was necessary due to the comparably small signal strength (maximum depletion upon photon absorption is on the order of 2%), and due to somewhat noisy signal counts, which had its origin in ion source instabilities caused by the sticky consistency of the methylamine precursor. Also, during the measurements, care was taken to avoid power broadening. Thus, the linewidths were expected to be dominated by the Doppler broadening due to the kinetic temperature of the ions in the trap (nominal temperature T = 4 K with some residual heating to typically 8 K), and a possible contribution due to non-resolved hyperfine splitting. The line patterns detected for a given rotational transition were in line with those expected for a prolate symmetric top molecule and at first sight, no further spectroscopic complexity, as could be expected for resolved nitrogen quadrupole hyperfine structure or torsional motion between the CH_3 and NH_3 subunits, was detected in individual measurements at our experimental conditions. For all individual measurements, the detected lines were fitted to Gaussian functions, from which line centers and their uncertainties were determined, and the first results were very similar to the frequencies quoted in **Table 2** (Model I).

The measured frequencies of the pure rotational lines collected in **Table 2** (Model I) were first fit with a standard symmetric rotor Hamiltonian using the PGOPHER program (Western, 2017), yielding the set of parameters for the ground state given in **Table 1** (fit I). Since the transitions of a symmetric rotor obey the ΔK = 0 selection rule, A and D_K cannot be determined experimentally, and only B_0, D_J and D_{JK} were derived in the least-squares fitting procedure and are presented in **Table 1**. Computed parameters are also included in **Table 1** for comparison. As can be seen, the overall agreement between the calculated and scaled best-estimate values and the experimental values is very good. A simulated stick spectrum and its convolution, based on fit I of **Table 1** and accounting for the hyperfine structure due to the quadrupole moment of the ^{14}N nucleus (with spin I = 1), are included in **Figure 1**. As the computed value eQq (^{14}N) = +158 kHz is very small (see also **Table 1**), it is not surprising that the hyperfine structure is not resolved in our experiment.

Closer inspection after co-addition of all spectra revealed some noticeable blue-shifted shoulders, as discernible in the accumulation of **Figure 1**. These are particularly evident in the spectra at 119 ($J = 3_K - 2_K$) and 159 GHz ($J = 4_K - 3_K$), but are also discernible in the weaker spectrum at 199 GHz ($J = 5_K - 4_K$). In the spectrum at 119 GHz (second panel in **Figure 1** and close-up in **Figure 2**) both blue shoulders have an offset of about +170 kHz relative to the main peaks (K = 0 and 1), and this offset is found to increase for the higher

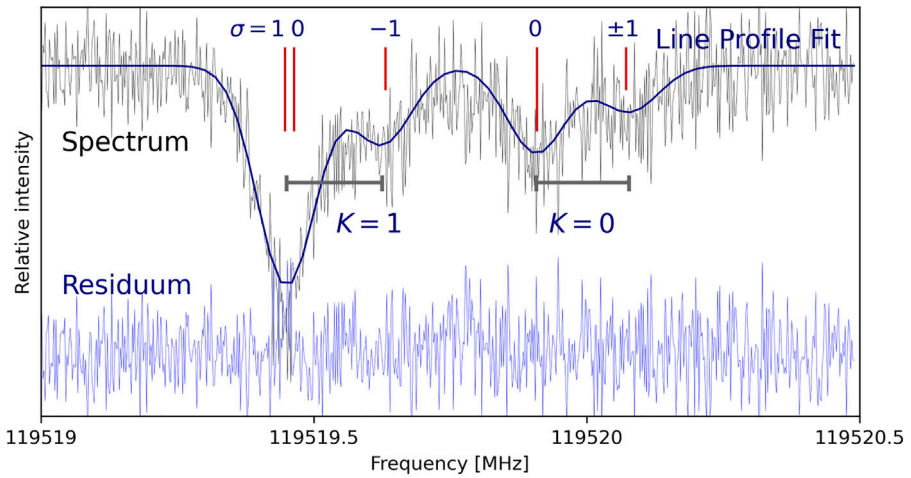

FIGURE 2 | Zoom into the transition $3_K \leftarrow 2_K$ ($K = 0, 1$) highlighting internal rotation splitting in $CH_3NH_3^+$. Four Gaussian features have been assumed in performing a line profile fit. The red vertical bars show the location of the five possible σ torsional components labeled at the top with the length of the bars indicating their contribution from spin statistical effects, see text for details. The gray horizontal markers indicate the torsional splitting of some 170 kHz observed in this particular transition (cf. transition frequencies collected in **Table 1**, Model II).

frequency transitions at 159 (≈+230 kHz) and 199 GHz (≈+290 kHz). While a detailed analysis is hampered by the overall poor signal-to-noise ratio of the spectra, a first analysis was performed here under the assumption that the spectra are affected by internal rotation, an effect that has rarely been observed previously for symmetric top molecules in their ground vibrational states (see, e.g., Ozier and Moazzen-Ahmadi, 2007, and references therein). As indicated in **Figure 2**, the structure of the $J = 3_K - 2_K$ spectrum may be decomposed into four features, two strong ones (the putative $K = 0$ and 1 components used in the first fitting procedure in **Table 1**, fit I) each of which is accompanied by a weaker satellite that is found blue-shifted relative to the main component. Similar patterns are observed for the $J = 4_K - 3_K$ and $J = 5_K - 4_K$ transitions. Ideally, a suitable model Hamiltonian should be able to reproduce both the magnitude of the torsional splitting as well as the intensities of the individual spectroscopic components. First, the magnitude of the torsional splitting to be expected in $CH_3NH_3^+$ was estimated based on the so-called *hybrid* approach described elsewhere (Wang et al., 2001) using the dominant parameters (V_3, $\rho = I_\alpha/I_c$, $F = A/(\rho \times (1 - \rho))$, F_{3J}, F_{3K}) as calculated here and complemented with parameters taken from isoelectronic ethane (Borvayeh et al., 2008). Using this approach, the splitting was predicted in very good agreement with the experimental values. In analogy to other closely related symmetric top molecules such as methyl silane, CH_3SiH_3, each rotational transition of $CH_3NH_3^+$ with $K = 1, 2$ is expected to split in up to three components ($\sigma = 0, +1, -1$) whereas transitions with $K = 0$ only split into two, $\sigma = 0, \pm1$ (Pelz et al., 1992; Ozier and Moazzen-Ahmadi, 2007). The symmetries and nuclear spin weights under consideration of torsional splitting that are needed for intensity estimates have been given, for example, in Pelz et al. (1992). From this, it is concluded that in the $CH_3NH_3^+$-spectra two strong torsional components of the $K = 1$-transitions ($\sigma = 0, 1$) are too close in frequency to be spectroscopically resolved and thus only one strong (superposition of $\sigma = 0$ and 1) and one weaker torsional component ($\sigma = -1$) are observed. The $K = 0$ splitting is also (partly) resolved and both components assigned, a stronger ($\sigma = 0$) and a weaker one ($\sigma = \pm1$), respectively. For the $K = 2$ transitions, only one component ($\sigma = 0$) can be assigned in the spectra obtained here with some confidence. Using this spectroscopic knowledge, the accumulated spectra as depicted in **Figure 1** were refitted using multiple Gaussian components, and the final frequencies and their assignments are listed in **Table 2**, Model II. With this improved spectroscopic assignment, a second fit was performed (using an in-house program and assuming a uniform frequency uncertainty of 15 kHz) leading to an alternative set of molecular parameters given in **Table 1** (fit II). In this approach, owing to the limited amount of spectroscopic information available to constrain the internal rotation problem more rigorously, several parameters required in the theoretical description were kept fixed at values calculated quantum-chemically (ρ, F, V_3). In analogy to fit I, B_0, D_J, and D_{JK} were varied in the least squares adjustment and additionally F_{3J} was released, resulting in a good fit result and agreement with the fit I and C_2H_6 parameter sets. If released also, V_3 cannot be determined statistically from the present data set and changing its value from the scaled calculated value of 2.42 kcal/mol to the unscaled value of 1.98 kcal/mol has little impact on the overall fit quality but decreases the value of F_{3J} significantly to −87(3) MHz. Based on this new set of parameters and taking into consideration the proper spin statistical effects (e.g., Pelz et al., 1992), new simulations of spectra have been obtained that are shown in **Figure 3**. The agreement between the experimental spectra and the simulations is rather compelling and hence speaking very much in favor of internal rotation as to the cause of the peculiar lineshapes and splittings observed.

5 INTERSTELLAR SEARCH

The $CH_3NH_3^+$ spectral line transitions reported in **Table 2** have frequencies > 40 GHz and constitute good targets to be searched

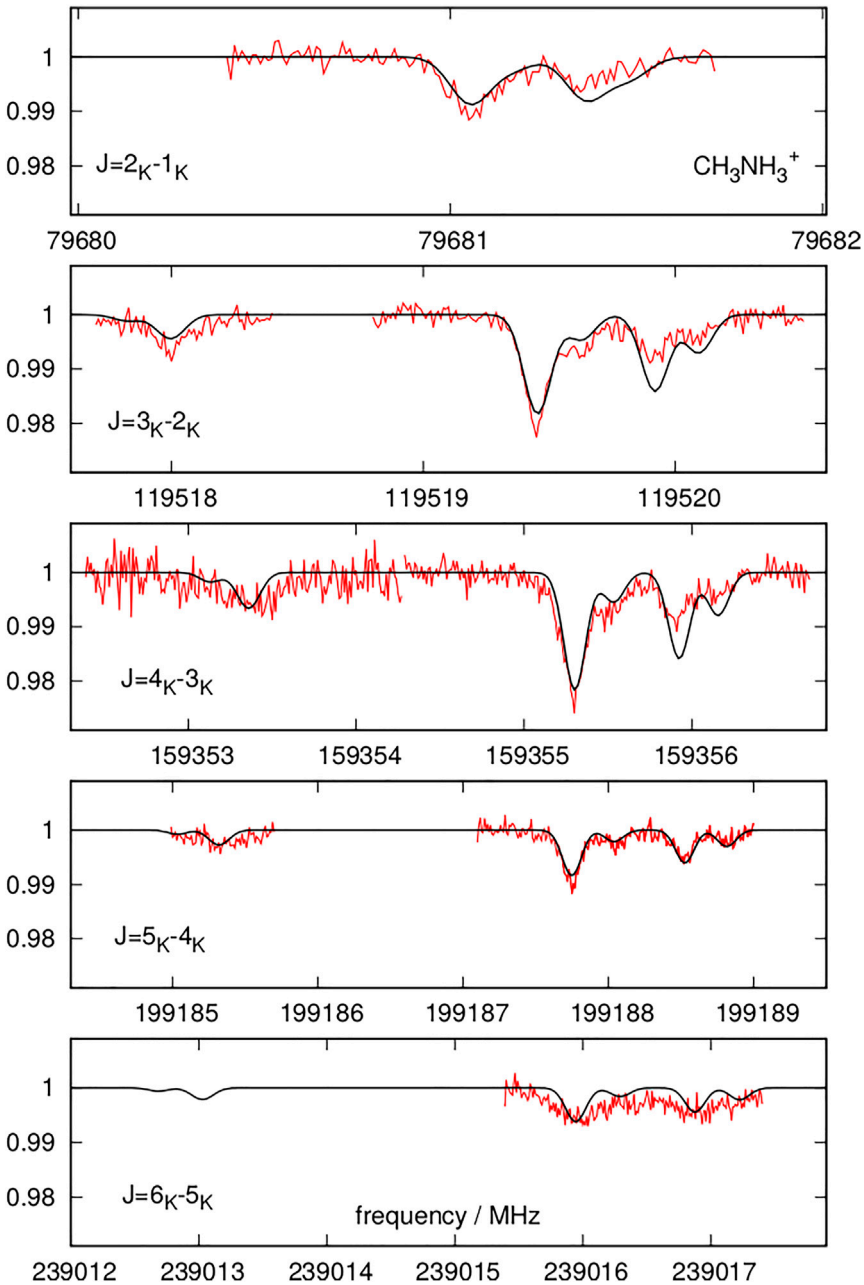

FIGURE 3 | Same as **Figure 1** but with torsional splitting included into the simulation (black line, **Table 1**, fit II). Owing to the very small magnitude of $eQq(^{14}N)$ calculated here, quadrupole hyperfine structure has not been considered in this simulation.

for with facilities like ALMA (Atacama Large Millimeter/submillimeter Array; ALMA Partnership et al., 2015). While the low-energy transitions are not covered by current ALMA bands, the $J = 4_K \rightarrow 3_K$ and $J_K = 5_K \rightarrow 4_K$ lines can be observed with the new ALMA band 5 receiver (covering a frequency range from 159 to 211 GHz), and the $J_K = 6_K \rightarrow 5_K$ transitions are observable with the commonly used band 6 receiver (211–276 GHz).

The detection of species closely related to protonated methylamine such as HCN, $HCNH^+$ or CH_3NH_2 in the star-forming region Sgr B2 (e.g., Schilke et al., 1991; Belloche et al., 2013) motivates the search for protonated methylamine in this region. We have made use of the ALMA spectral line survey published in Sánchez-Monge et al. (2017, see also Schwörer et al., 2019). The observations target the star-forming objects Sgr B2(N) and Sgr B2(M) and cover the whole ALMA band 6 with a spectral resolution of 0.7 km s^{-1} and an angular resolution of 0.″4 (corresponding to 3300 au at the distance of the source). This high angular resolution allows to resolve the regions in more than 40 different dense cores (see Sánchez-Monge et al., 2017). **Figure 4** presents the spectra extracted

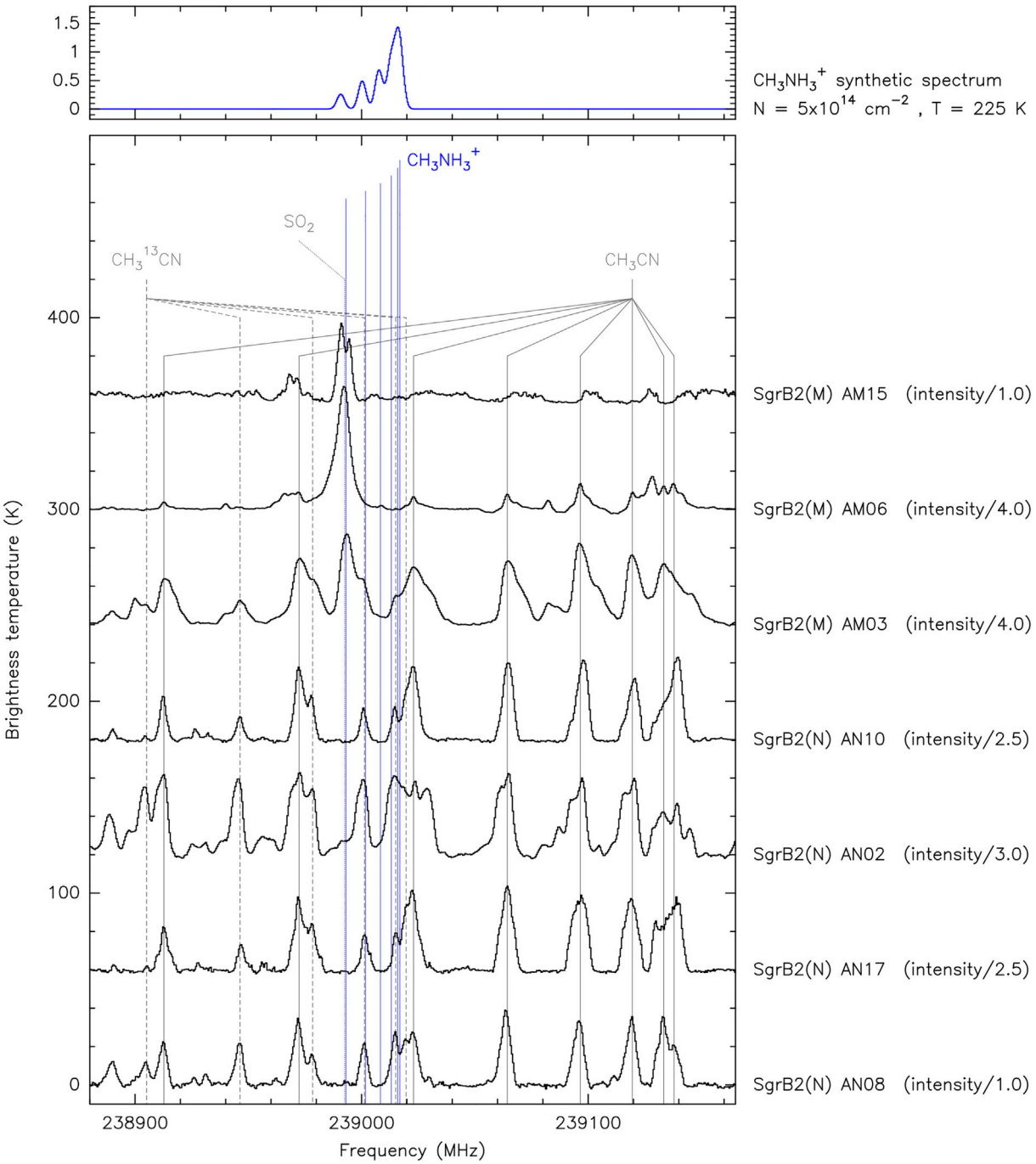

FIGURE 4 | ALMA spectra towards seven dense cores in the Sgr B2(N) and (M) regions. Data from Sánchez-Monge et al. (2017). The baseline for each spectrum corresponds to a brightness temperature of 0 K, however, the spectrum of each source has been manually shifted by 60 K (with respect to the source below) for an easier visualization of the data. The intensities of some spectra have been divided by the factor indicated to the right. Grey solid and dashed vertical lines mark the transitions of CH_3CN ($J_K = 13_K - 12_K$), $CH_3^{13}CN$ ($J_K = 13_K - 12_K$) and SO_2 ($J_{K_a,K_c} = 21_{7,15} - 22_{6,16}$). The blue vertical lines mark the $6_K \rightarrow 5_K$ transitions of $CH_3NH_3^+$. The top panel shows the expected synthetic spectrum for $CH_3NH_3^+$ as observed with ALMA at 0.″4 angular resolution and considering a column density of 5×10^{14} cm^{-2}, a temperature of 225 K, and a linewidth of 5 km s^{-1}.

towards different selected cores in both regions (see source coordinates in **Tables 1**, **2** of Sánchez-Monge et al., 2017). The spectra are obtained after averaging the emission inside the 3σ polygon that defines the source size (between 0.″5 and 0.″7). We mark with vertical lines the location of the $CH_3NH_3^+$ transitions.

We have selected objects in different evolutionary stages and with different physical properties. Cores AN02, AN17 and AM03

correspond to dense cores dominated by dust but with a rich chemistry. In particular, core AN02 has been extensively studied in the literature in the search of new chemical species (e.g., Belloche et al., 2014). We have also included objects in which an embedded HII region has been found (e.g., AN10, AM06, AM15). The presence of the UV radiation from embedded massive stars ionizing the gas and resulting in HII regions can enhance the protonation of methylamine in the photon-dominated region around the HII region. As shown in **Figure 4**, no obvious features are detected at the frequencies of the tabulated $CH_3NH_3^+$ transitions, suggesting a low abundance of protonated methylamine in Sgr B2. We have determined an upper limit of $\approx 5 \times 10^{14}$ cm^{-2} to the column density of protonated methylamine. This is estimated based on a 3-sigma noise upper limit and assuming a gas temperature of 200–300 K (as derived from other molecular species in Sgr B2, Schwörer et al., 2019). This translates into an upper limit of the fractional abundance of ~10^{-10}. The high densities of the Sgr B2 region (~ 10^5–10^8 cm^{-3}; see also Schmiedeke et al., 2016) can rapidly attenuate the radiation field and result in a low production of heavy ions like $CH_3NH_3^+$. Moreover, the $J = 6_K \rightarrow 5_K$ transitions are located close to bright CH_3CN and $CH_3^{13}CN$ ($J_K = 13_K \rightarrow 12_K$) transitions and a strong SO_2 feature which may hinder the detection of the weaker $CH_3NH_3^+$ in chemically rich, embedded objects. Observations at other frequency ranges, as well as in other astronomical sources associated with highly ionized and less dense gas, may help in the detection of this species in space.

6 CONCLUSION AND OUTLOOK

In the present study, the pure rotational spectrum of protonated methyl amine, $CH_3NH_3^+$, was observed for the first time. It is worthwhile to recall that upon protonation of CH_3NH_2, forming $CH_3NH_3^+$, the complex dynamical behaviour of the former molecular system is largely simplified, because the inversion at the NH_2 group in CH_3NH_2 is eliminated and only the torsional motion between CH_3 and NH_3 has to be potentially considered for the pure rotational spectrum of $CH_3NH_3^+$ in its ground vibrational state. In this study, a total of five pure rotational transitions from $J = 2_K - 1_K$ to $J = 6_K - 5_K$ and K up to 2 were identified. As indicated through complementary quantum-chemical calculations, explicit treatment of nuclear quadrupole hyperfine structure from the presence of the nitrogen nucleus was found to be negligible. While the strongest spectroscopic features in the spectrum can be assigned and fitted reasonably well in a straightforward fashion using a standard symmetric-top Hamiltonian, peculiar lineshapes and weak substructure identified in the spectra upon close inspection indeed required extension of the theoretical treatment to account for internal rotation. This refined model description permits very convincing reproduction of the experimental line profiles. A more comprehensive treatment of the internal rotational problem in $CH_3NH_3^+$ would certainly benefit from extension of the present work to a higher degree of rotational excitation but also from detection of vibrational satellites of $CH_3NH_3^+$ in torsionally excited states.

Future work towards the spectroscopic characterization of protonated amines offers many possibilities, not only in the millimeter-wave regime. For example, the low-resolution vibrational spectra of $CH_3NH_3^+$ and also protonated ethyl amine, $C_2H_5NH_3^+$, were observed recently in the range from 700 to 1750 cm^{-1} (Thorwirth et al., 2019b) using the FELion ion trap apparatus (Jusko et al., 2019). For the purpose of millimeter-wave radio astronomical searches of $CH_3NH_3^+$ the data presented here should already suffice. Although the column density of $CH_3NH_3^+$ in the interstellar medium may be some orders of magnitude lower than that of CH_3NH_2, the more favorable partition function of $CH_3NH_3^+$ will support radio astronomical detectability. In the search towards SgrB2 presented in this work $CH_3NH_3^+$ was unfortunately not found.

DATA AVAILABILITY STATEMENT

The raw data supporting the conclusion of this article will be made available by the authors, without undue reservation.

AUTHOR CONTRIBUTIONS

PS: measurement, manuscript writing MT: measurement ST: quantum chemical computations, data evaluation, manuscript writing CE: data evaluation, manuscript writing AS-M: data evaluation, manuscript writing AS: data evaluation, manuscript writing PS: supervision SS: supervision, manuscript writing OA: measurement, data evaluation, manuscript writing, supervision.

FUNDING

This work has been supported via Collaborative Research Centre 956, sub-projects A6 and B2, funded by the Deutsche Forschungsgemeinschaft (DFG, project ID 184 018 867), as well as DFG SCHL 341/15-1 (Gerätezentrum “Cologne Center for Terahertz Spectroscopy”).

ACKNOWLEDGMENTS

The authors gratefully acknowledge the work done over the last years by the electrical and mechanical workshops of the I. Physikalisches Institut. We thank Frank Lewen for assistance using the mm-wave setup. CE is grateful for support from the Max Planck Society.

SUPPLEMENTARY MATERIAL

The Supplementary Material for this article can be found online at: https://www.frontiersin.org/articles/10.3389/fspas.2021.805162/full#supplementary-material

REFERENCES

Asvany, O., Bielau, F., Moratschke, D., Krause, J., and Schlemmer, S. (2010). Note: New Design of a Cryogenic Linear Radio Frequency Multipole Trap. *Rev. Sci. Instrum.* 81, 076102. doi:10.1063/1.3460265

Asvany, O., Brünken, S., Kluge, L., and Schlemmer, S. (2014). COLTRAP: A 22-pole Ion Trapping Machine for Spectroscopy at 4 K. *Appl. Phys. B* 114, 203–211. doi:10.1007/s00340-013-5684-y

Asvany, O., Krieg, J., and Schlemmer, S. (2012). Frequency Comb Assisted Mid-Infrared Spectroscopy of Cold Molecular Ions. *Rev. Sci. Instrum.* 83, 093110. doi:10.1063/1.4753930

Asvany, O., Markus, C. R., Roucou, A., Schlemmer, S., Thorwirth, S., and Lauzin, C. (2021). The Fundamental Rotational Transition of NO^+. *J. Mol. Spectrosc.* 378, 111447. doi:10.1016/j.jms.2021.111447

Asvany, O., Yamada, K. M. T., Brünken, S., Potapov, A., and Schlemmer, S. (2015). Experimental Ground-State Combination Differences of CH_5^+. *Science* 347, 1346–1349. doi:10.1126/science.aaa3304

Belloche, A., Garrod, R. T., Müller, H. S. P., and Menten, K. M. (2014). Detection of a Branched Alkyl Molecule in the Interstellar Medium: Iso-Propyl Cyanide. *Science* 345, 1584–1587. doi:10.1126/science.1256678

Belloche, A., Müller, H. S. P., Menten, K. M., Schilke, P., and Comito, C. (2013). Complex Organic Molecules in the Interstellar Medium: IRAM 30 m Line Survey of Sagittarius B2(N) and (M). *Astron. Astrophys.* 559, A47. doi:10.1051/0004-6361/201321096

Borvayeh, L., Moazzen-Ahmadi, N., and Horneman, V.-M. (2008). The $\nu_{12} - \nu_9$ Band of Ethane: A Global Frequency Analysis of Data from the Four Lowest Vibrational States. *J. Mol. Spectrosc.* 250, 51–56. doi:10.1016/j.jms.2008.04.009

Brünken, S., Kluge, L., Stoffels, A., Asvany, O., and Schlemmer, S. (2014). Laboratory Rotational Spectrum of l-C_3H^+ and Confirmation of its Astronomical Detection. *Astrophys. J. Lett.* 783, L4. doi:10.1088/2041-8205/783/1/l4

Brünken, S., Kluge, L., Stoffels, A., Pérez-Ríos, J., and Schlemmer, S. (2017). Rotational State-dependent Attachment of He Atoms to Cold Molecular Ions: An Action Spectroscopic Scheme for Rotational Spectroscopy. *J. Mol. Spectrosc.* 332, 67–78. doi:10.1016/j.jms.2016.10.018

Buhl, D., and Snyder, L. E. (1970). Unidentified Interstellar Microwave Line. *Nature* 228, 267–269. doi:10.1038/228267a0

Doménech, J. L., Jusko, P., Schlemmer, S., and Asvany, O. (2018a). The First Laboratory Detection of Vibration-Rotation Transitions of $^{12}CH^+$ and $^{13}CH^+$ and Improved Measurement of Their Rotational Transition Frequencies. *Astrophys. J.* 857, 61. doi:10.3847/1538-4357/aab36a

Doménech, J. L., Schlemmer, S., and Asvany, O. (2017). Accurate Frequency Determination of Vibration-Rotation and Rotational Transitions of SiH^+. *Astrophys. J.* 849, 60. doi:10.3847/1538-4357/aa8fca

Doménech, J. L., Schlemmer, S., and Asvany, O. (2018b). Accurate Rotational Rest Frequencies for Ammonium Ion Isotopologues. *Astrophys. J.* 866, 158. doi:10.3847/1538-4357/aadf83

Dunning, T. H. (1989). Gaussian Basis Sets for Use in Correlated Molecular Calculations. I. The Atoms Boron through Neon and Hydrogen. *J. Chem. Phys.* 90, 1007–1023. doi:10.1063/1.456153

ALMA PartnershipFomalont, E. B., Vlahakis, C., Corder, S., Remijan, A., Barkats, D., et al. (2015). The 2014 ALMA Long Baseline Campaign: An Overview. *Astrophys. J. Lett.* 808, L1. doi:10.1088/2041-8205/808/1/L1

Fourikis, N., Takagi, K., and Morimoto, M. (1974). Detection of Interstellar Methylamine by its $2_{02} \rightarrow 1_{10}$ A_a-State Transition. *Astrophys. J. Lett.* 191, L139. doi:10.1086/181570

Gauss, J., and Stanton, J. F. (1997). Analytic CCSD(T) Second Derivatives. *Chem. Phys. Lett.* 276, 70–77. doi:10.1016/s0009-2614(97)88036-0

Godfrey, P. D., Brown, R. D., Robinson, B. J., and Sinclair, M. W. (1973). Discovery of Interstellar Methanimine (Formaldimine). *Astrophys. Lett.* 13, 119.

Herbst, E. (1985). The Rate of the Radiative Association Reaction between CH_3^+ and NH_3 and its Implications for Interstellar Chemistry. *Astrophys. J.* 292, 484–486. doi:10.1086/163179

Ilyushin, V., and Lovas, F. J. (2007). Microwave Spectra of Molecules of Astrophysical Interest. Xxv. Methylamine. *J. Phys. Chem. Ref. Data* 36, 1141–1276. doi:10.1063/1.2769382

Jusko, P., Brünken, S., Asvany, O., Thorwirth, S., Stoffels, A., van der Meer, L., et al. (2019). The FELion Cryogenic Ion Trap Beam Line at the FELIX Free-Electron Laser Laboratory: Infrared Signatures of Primary Alcohol Cations. *Faraday Discuss.* 217, 172–202. doi:10.1039/c8fd00225h

Jusko, P., Stoffels, A., Thorwirth, S., Brünken, S., Schlemmer, S., and Asvany, O. (2017). High-resolution Vibrational and Rotational Spectroscopy of CD_2H^+ in a Cryogenic Ion Trap. *J. Mol. Spectrosc.* 332, 59–66. doi:10.1016/j.jms.2016.10.017

Kaifu, N., Morimoto, M., Nagane, K., Akabane, K., Iguchi, T., and Takagi, K. (1974). Detection of Interstellar Methylamine. *Astrophys. J. Lett.* 191, L135–L137. doi:10.1086/181569

Markus, C. R., Thorwirth, S., Asvany, O., and Schlemmer, S. (2019). High-Resolution Double Resonance Action Spectroscopy in Ion Traps: Vibrational and Rotational Fingerprints of $CH_2NH_2^+$. *Phys. Chem. Chem. Phys.* 21, 26406–26412. doi:10.1039/c9cp05487a

Martinez, O., Jr., Lattanzi, V., Thorwirth, S., and McCarthy, M. C. (2013). Detection of Protonated Vinyl Cyanide, CH_2CHCNH^+, a Prototypical Branched Nitrile Cation. *J. Chem. Phys.* 138, 094316. doi:10.1063/1.4793316

Matthews, D. A., Cheng, L., Harding, M. E., Lipparini, F., Stopkowicz, S., Jagau, T.-C., et al. (2020). Coupled-Cluster Techniques for Computational Chemistry: The CFOUR Program Package. *J. Chem. Phys.* 152, 214108. doi:10.1063/5.0004837

McKellar, A. (1940). Evidence for the Molecular Origin of Some Hitherto Unidentified Interstellar Lines. *Publ. Astron. Soc. Pac.* 52, 187. doi:10.1086/125159

Michi, T., Ohashi, K., Inokuchi, Y., Nishi, N., and Sekiya, H. (2003). Infrared Spectra and Structures of $(CH_3NH_2)_nH^+$ (n = 1-4). Binding Features of an Excess Proton. *Chem. Phys. Lett.* 371, 111–117. doi:10.1016/s0009-2614(03)00217-3

Motiyenko, R. A., Ilyushin, V. V., Drouin, B. J., Yu, S., and Margulès, L. (2014). Rotational Spectroscopy of Methylamine up to 2.6 THz. *Astron. Astrophys.* 563, A137. doi:10.1051/0004-6361/201323190

Ohashi, N., Takagi, K., Hougen, J. T., Olson, W. B., and Lafferty, W. J. (1987). Far-Infrared Spectrum and Ground State Constants of Methyl Amine. *J. Mol. Spectrosc.* 126, 443–459. doi:10.1016/0022-2852(87)90249-9

Ozier, I., and Moazzen-Ahmadi, N. (2007). "Internal Rotation in Symmetric Tops," in *Advances in Atomic, Molecular, and Optical Physics*. Editors P. R. Berman, C. C. Lin, and E. Arimondo (Amsterdam: Elsevier), 54, 423–509. doi:10.1016/s1049-250x(06)54007-8

Pelz, G., Mittler, P., Yamada, K. M. T., and Winnewisser, G. (1992). Millimeter-Wave Spectra and Revised Spectroscopic Parameters of Methylsilane. *J. Mol. Spectrosc.* 156, 390–402. doi:10.1016/0022-2852(92)90240-o

Peterson, K. A., and Dunning, T. H. (2002). Accurate Correlation Consistent Basis Sets for Molecular Core-Valence Correlation Effects: The Second Row Atoms Al-Ar, and the First Row Atoms B-Ne Revisited. *J. Chem. Phys.* 117, 10548–10560. doi:10.1063/1.1520138

Puzzarini, C., Stanton, J. F., and Gauss, J. (2010). Quantum-Chemical Calculation of Spectroscopic Parameters for Rotational Spectroscopy. *Int. Rev. Phys. Chem.* 29, 273–367. doi:10.1080/01442351003643401

Raghavachari, K., Trucks, G. W., Pople, J. A., and Head-Gordon, M. (1989). A Fifth-Order Perturbation Comparison of Electron Correlation Theories. *Chem. Phys. Lett.* 157, 479–483. doi:10.1016/s0009-2614(89)87395-6

Sánchez-Monge, Á., Schilke, P., Schmiedeke, A., Ginsburg, A., Cesaroni, R., Lis, D. C., et al. (2017). The Physical and Chemical Structure of Sagittarius B2. II. Continuum Millimeter Emission of Sgr B2(M) and Sgr B2(N) with ALMA. *Astron. Astrophys.* 604, A6. doi:10.1051/0004-6361/201730426

Schilke, P., Walmsley, C. M., Millar, T. J., and Henkel, C. (1991). Protonated HCN in Molecular Clouds. *Astron. Astrophys.* 247, 487.

Schmiedeke, A., Schilke, P., Möller, T., Sánchez-Monge, Á., Bergin, E., Comito, C., et al. (2016). The Physical and Chemical Structure of Sagittarius B2. I. Three-Dimensional Thermal Dust and Free-Free Continuum Modeling on 100 au to 45 pc Scales. *Astron. Astrophys.* 588, A143. doi:10.1051/0004-6361/201527311

Schwörer, A., Sánchez-Monge, Á., Schilke, P., Möller, T., Ginsburg, A., Meng, F., et al. (2019). The Physical and Chemical Structure of Sagittarius B2. IV. Converging Filaments in the High-Mass Cluster Forming Region Sgr B2(N). *Astron. Astrophys.* 628, A6. doi:10.1051/0004-6361/201935200

Snyder, L. E., and Buhl, D. (1972). Detection of Several New Interstellar Molecules. *Ann. N. Y. Acad. Sci.* 194, 17–24. doi:10.1111/j.1749-6632.1972.tb12687.x

Snyder, L. E., and Buhl, D. (1971). Observations of Radio Emission from Interstellar Hydrogen Cyanide. *Astrophys. J. Lett.* 163, L47. doi:10.1086/180664

Stanton, J. F., and Gauss, J. (2000). Analytic Second Derivatives in High-Order many-body Perturbation and Coupled-Cluster Theories: Computational Considerations and Applications. *Int. Rev. Phys. Chem.* 19, 61–95. doi:10.1080/014423500229864

Stanton, J. F., Lopreore, C. L., and Gauss, J. (1998). The Equilibrium Structure and Fundamental Vibrational Frequencies of Dioxirane. *J. Chem. Phys.* 108, 7190–7196. doi:10.1063/1.476136

Thaddeus, P., Guélin, M., and Linke, R. A. (1981). Three New 'nonterrestrial' Molecules. *Astrophys. J.* 246, L41–L45. doi:10.1086/183549

Thorwirth, S., Schreier, P., Salomon, T., Schlemmer, S., and Asvany, O. (2019a). Pure Rotational Spectrum of CN^+. *Astrophys. J. Lett.* 882, L6. doi:10.3847/2041-8213/ab3927

Thorwirth, S., Schmid, P. C., Töpfer, M., Brünken, S., Asvany, O., and Schlemmer, S. (2019b). "Spectroscopic Studies of Protonated Amines: $CH_3NH_3^+$ and $C_2H_5NH_3^+$," in International Symposium on Molecular Spectroscopy, 74th meeting, Champaign-Urbana, IL, U.S.A., June 17-21, Talk WF04.

Turner, B. E. (1974). U93.174 - A New Interstellar Line with Quadrupole Hyperfine Splitting. *Astrophys. J. Lett.* 193, L83. doi:10.1086/181638

Wakelam, V., Loison, J. C., Herbst, E., Pavone, B., Bergeat, A., Beroff, K., et al. (2015). The 2014 KIDA Network for Interstellar Chemistry. *Astrophys. J. Suppl. Ser.* 217, 20. doi:10.1088/0067-0049/217/2/20

Wang, S.-X., Schroderus, J., Ozier, I., Moazzen-Ahmadi, N., McKellar, A. R. W., Ilyushyn, V. V., et al. (2001). Infrared and Millimeter-Wave Study of the Four Lowest Torsional States of CH_3CF_3. *J. Mol. Spectrosc.* 205, 146–163. doi:10.1006/jmsp.2000.8235

Watts, J. D., Gauss, J., and Bartlett, R. J. (1992). Open-Shell Analytical Energy Gradients for Triple Excitation many-body, Coupled-Cluster Methods: MBPT(4), CCSD+T(CCSD), CCSD(T), and QCISD(T). *Chem. Phys. Lett.* 200, 1–7. doi:10.1016/0009-2614(92)87036-o

Western, C. M. (2017). Pgopher: A Program for Simulating Rotational, Vibrational and Electronic Spectra. *J. Quant. Spectrosc. Radiat. Transf.* 186, 221–242. doi:10.1016/j.jqsrt.2016.04.010

Zeroka, D., and Jensen, J. O. (1998). Infrared Spectra of Some Isotopomers of Methylamine and the Methylammonium Ion: A Theoretical Study. *J. Mol. Struct. THEOCHEM* 425, 181–192. doi:10.1016/s0166-1280(97)00109-7

Ziurys, L. M., and Turner, B. E. (1986). HCNH(+) - A New Interstellar Molecular Ion. *Astrophys. J.* 302, L31–L36. doi:10.1086/184631

Zuckerman, B., Morris, M., Palmer, P., and Turner, B. E. (1972). Observations of Cs, HCN, U89.2, and U90.7 in NGC 2264. *Astrophys. J. Lett.* 173, L125. doi:10.1086/180931

Conflict of Interest: The authors declare that the research was conducted in the absence of any commercial or financial relationships that could be construed as a potential conflict of interest.

Publisher's Note: All claims expressed in this article are solely those of the authors and do not necessarily represent those of their affiliated organizations, or those of the publisher, the editors and the reviewers. Any product that may be evaluated in this article, or claim that may be made by its manufacturer, is not guaranteed or endorsed by the publisher.